

Nucleation of *c*-BN on hexagonal boron nitride

B. Mårilid, K. Larsson, and J.-O. Carlsson

Department of Materials Chemistry, The Ångström Laboratory, Uppsala University, Box 538, S-751 21 Uppsala, Sweden

(Received 21 August 2000; revised manuscript received 5 February 2001; published 18 October 2001)

The nucleation of cubic boron nitride (*c*-BN) on the zigzag edges (100) and $\bar{1}00$, as well as on the armchair edge (110) of the basal (001) plane of hexagonal BN (*h*-BN) has been theoretically investigated, using a cluster approach and the density-functional theory. The total energy of the different buckled (cubic and wurtzitic) outgrowths from the edge atoms has then been related to the total energy of the corresponding planar (hexagonal) counterparts. The different outgrowths, as well as the various types of edge atoms, were all terminated with H or F atoms. For the zigzag edges it was shown that the nucleation of *c*-BN is the energetically most favorable one in an H- or F-rich environment. On the armchair edge, however, the nucleation of wurtzitic BN (*w*-BN) was even more energetically preferred. Furthermore, it was shown that the F atoms possess a significantly larger ability to stabilize the *c*-BN nuclei than do the H atoms.

DOI: 10.1103/PhysRevB.64.184107

PACS number(s): 82.65.+r

I. INTRODUCTION

Deposition techniques for growth of boron nitride (BN) thin films can roughly be divided into either of two routes, the “physical” or the “chemical” route.¹ The physical route involves mainly physical vapor deposition (PVD) methods with surface bombardment of highly energetic nitrogen and/or argon ions.^{2–4} BN films deposited by these methods often suffer from poor adhesion and cracking due to large compressive stresses caused by the ion bombardment. PVD films usually consist of a layer of amorphous BN next to the substrate, followed by a hexagonal BN (*h*-BN) layer, and finally followed by a very thin top layer of *c*-BN.⁵ In addition, sp^2 -hybridized BN has, with ion plating and ion-beam-assisted deposition, been found in the grain boundaries of polycrystalline *c*-BN,^{6,7} as well as on top of *c*-BN grains (with a thickness of about 3 ML).⁸ The chemical route on the other hand, comprises thermally activated, hot-filament-assisted, and hydrogen plasma-enhanced chemical vapor deposition (TACVD), (HFCVD), and (PECVD), respectively. Using TACVD (or HFCVD) the films presently become a multiphase mixture of the following phases: amorphous (*a*-BN), turbostratic, poorly crystallized sp^2 -hybridized BN (*t*-BN), and *h*-BN.^{9–11} In hydrogen PECVD, BN films have been deposited with a large fraction of the cubic phase. The cubic BN is then formed as crystallites codeposited with a mixture of *a*-BN and/or *h*-BN.^{1,12} Based on results from a rf-sputtering process (PVD), it has been observed that the cubic BN crystallites are nucleating on the edges of the *h*-BN planes in such a way that the *c*-BN [111] is normal to the *h*-BN [002] (*c* axis).¹³ Common for the “physical” and “chemical” routes is, hence, the involvement of sp^2 -hybridized BN. As presented above, it either functions as a “substrate” for *c*-BN growth (in PVD and PECVD) or as the actual resulting film (in TACVD and HFCVD). In order to produce films with good adhesion, the growth of a heteroepitaxial (or textured) *c*-BN film directly on the substrate or via a highly oriented *h*-BN conversion layer (without the amorphous layer) is of great importance. Although

the growth of *c*-BN directly onto a silicon substrate has not been reported, well-adhered and highly oriented *h*-BN or *c*-BN films on Si have been observed, with only turbostratic BN as a conversion layer.^{2,14} It is, thus, for two reasons important to carefully study the nucleation stage in *c*-BN thin-film formation, first, to gain a deeper knowledge of the nucleation process of *c*-BN on *h*-BN, and second, to improve the control of the nucleation process.

It has been observed in a recent paper by the present authors that surface B (or N) atoms on the basal plane of *h*-BN will become sp^3 -hybridized upon adsorption of H or F.¹⁵ As a result, the adsorbed atom [together with the surface B (or N) atom] will become somewhat uplifted from the surface, hence forming an “embryonic” *c*-BN nucleus. As a natural continuation of this previous study, the possibility for nucleation of *c*-BN on also the edge atoms of *h*-BN (001) is of great interest to investigate. The purpose of the present work is therefore to make a comparative structural and energetic theoretical investigation of *c*-BN nucleation on the three different edges of the *h*-BN (001) plane, using a cluster approach and the density-functional theory (DFT).^{16,17} The three edges include two zigzag edges [boron atoms on the (100) edge and nitrogen atoms on the $\bar{1}00$ edge] and the armchair edge [a combination of boron and nitrogen atoms on the (110) edge] (Fig. 1). The stability of sp^3 -hybridized BN outgrowths (H or F terminated) will then be presented and discussed in relation to a continued growth of *h*-BN.

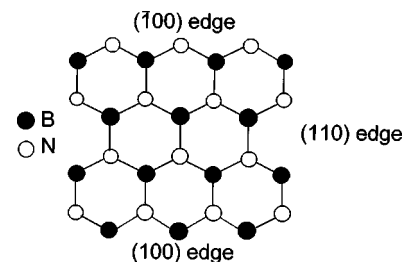


FIG. 1. A model of a nonterminated *h*-BN (001) basal plane, demonstrating the $\bar{1}00$, (100), and (110) edges, respectively.

II. METHOD

The nucleation of cubic boron nitride on the zigzag and armchair edge atoms of the *h*-BN(001) plane has been investigated within density-functional theory,^{16,17} using the program system DMOL (from Accelrys, Inc., San Diego) and a cluster approach. The local-density approximation (LDA) is one of the earliest approximations in DFT. It includes correction for electron correlation effects. However, one of the most important deficiencies with the LDA exchange, the incorrect asymptotic behavior, leads numerically to an overestimated chemical bond energy for the system. This can be solved by using various types of generalized gradient approximations (GGA's); Becke-Lee, Yang, and Parr (B-LYP), Beck and Perdew-Wang (BP), Perdew and Wang, 1991 (PW91), and Vosko, Wilk, and Nusair-Becke and Perdew-Wang (VWN-BP), etc. The B-LYP functional contains the local Dirac LDA_x plus Becke's 1988 gradient-corrected exchange functional (B88_x) (Ref. 18) in combination with the gradient-corrected correlation functional by Lee, Yang and Parr (LYP_c).¹⁹ The BP functional is a combination of the B88_x functional and the Perdew and Wang correlation functional (PW_c).²⁰ Instead of using the LYP_c functional, the Dirac LDA_x plus Becke's B88_x correction has here been connected with the Perdew and Wang 1991 correlation functional, which is based on a slowly varying electron density.²¹ The PW91 functional consists of the Dirac LDA_x functional and the gradient-corrected PW91 correlation functional and is entirely free of empirical parameters.²² And, finally, in the VWN-BP functional (which is similar to the BP functional), the local correlation functional PW_c is replaced by the local correlation functional VWN.

For comparison purposes, the atomization energy of *c*-BN has been calculated using the four different GGA functionals presented above. These numerical values were then compared with an experimentally obtained one for BN.²³ The average error obtained when using the LDA functionals was 89 kJ/mol. The introduction of gradient corrections dramatically improved the situation. The corresponding average error for the GGA methods was 14 kJ/mol [B-LYP (384), BP (383), PW91 (410), VWN-BP (415), and experimental (392)]. Hence, the best accuracy compared to experiment was obtained by using the functionals BP and B-LYP. Total energies and geometrical structures were therefore in the present investigation calculated using the first-principles local-density approximation in combination with the nonlocal gradient-corrected functional B-LYP. The present work includes calculations of the total electronic energies for two different types of outgrowths on the three edges: *sp*³-hybridized BN systems (representing the cubic and wurtzitic phase) and the *sp*²-hybridized planar hexagonal counterpart. The outgrowths are then either H or F terminated.

To calculate the stabilization of the buckled (*c*-BN or *w*-BN) outgrowth in relation to the planar (*h*-BN) counterpart, the following formula was used:

$$\Delta E = E_{\text{planar}} - E_{\text{buckled}} + nE_X, \quad (1)$$

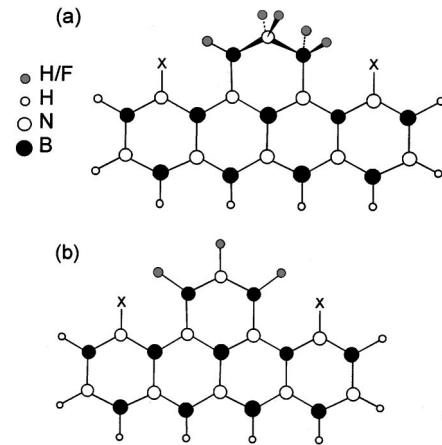


FIG. 2. An illustration of (a) *c*-BN and (b) *h*-BN nucleation on a template modeling the (100) edge of the *h*-BN (001) plane. The gray atoms are either terminating H or F species. The terminating species “X” (neighboring the outgrowth) are either H or F.

where E_{planar} and E_{buckled} are the calculated total energies for the planar and buckled outgrowths, respectively, and E_X is the total energy for an H or F atom (depending on the type of termination of the outgrowth). The relative energies have to be balanced by the difference in the number of terminating species (n) for the planar and buckled outgrowths.

A necessary condition for obtaining a good description of the electronic state of the systems of interest is to choose a highly flexible basis set and a model cluster adequately describing the *h*-BN surface plane. Geometry optimizations are also of great importance. A double numeric basis set with polarization (DNP) functions has been used in the present investigation. The DNP basis set is corresponding to the commonly used Gaussian analytical basis set, 6–31 G^{**}.²⁴ This basis set is suitable for polar compounds like BN since it is improved, compared to the minimal basis set, in the description of expansions and contractions of the valence shell in response to different molecular environments. It also adequately describes charge rearrangements around the atoms.

A previous study of diamond nucleation on *h*-BN showed that a template of the size $B_7N_7H_8$ was sufficient in modeling nucleation on the (110) edge of the (001) plane of *h*-BN.²⁵ When including the effect of neighboring terminating species (to the outgrowths), it was later shown to be more adequate to use a slightly larger template ($B_9N_9H_{10}$).^{26,27} The presence of substituents on both sides of the outgrowth implies a template consisting of at least four aligned aromatic B_3N_3 rings, with the two central rings carrying the outgrowth and the two outer rings with the terminated edge atoms (Fig. 2). In modeling the *h*-BN(001) plane edges in the present investigation, the larger template size ($B_9N_9H_{10}$) will be used for the two (100) and $(\bar{1}00)$ edges and the smaller one ($B_7N_7H_8$) for the (110) edge. The edge atoms are H terminated through adsorption of atomic hydrogen from the gaseous phase, which has been shown to be energetically favored for graphite sheets.²⁸

To adequately simulate the bulk material of *h*-BN, the experimental B-N bond length (1.446 Å) (Ref. 29) is chosen.

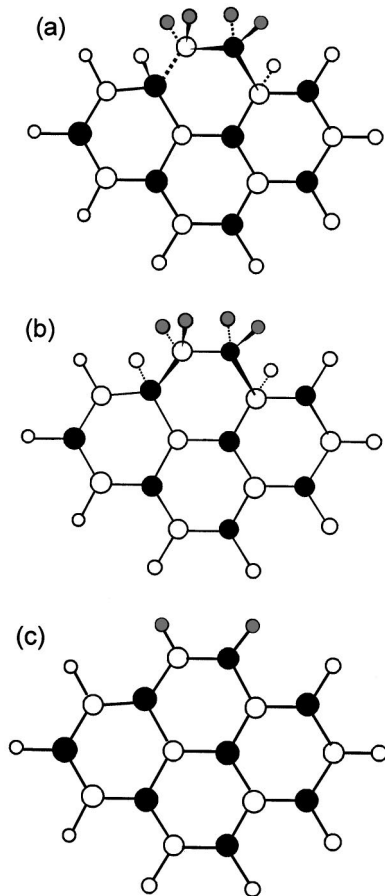


FIG. 3. A model representing BN nucleation on the (110) edge of the basal plane of *h*-BN. The (a) chair configuration corresponds to cubic BN nucleation, while the (b) boat conformation corresponds to nucleation of wurtzitic BN. The (c) planar configuration corresponds to a continued growth of *h*-BN. The gray atoms are either terminating H or F species.

Moreover, the buckled outgrowths (*c*-BN or *w*-BN nuclei) on the (100) and $\bar{1}00$ edges consist of three saturated atoms, and the planar counterparts (*h*-BN nuclei) consist of three nonsaturated atoms (Fig. 2). On the (110) edge, the buckled outgrowth is composed of two saturated atoms and the planar of two sp^2 -hybridized atoms (Fig. 3). All geometrical parameters for the different BN outgrowths, as well as the two edge atoms bonded to these outgrowths, were allowed to be fully relaxed. All other atoms were kept fixed in order to hold the characteristics of the crystal.

III. MODEL CLUSTER SIZE EFFECTS

When modeling a realistic crystalline surface, a two-dimensional slab or cluster template is often used. Upon reducing dimensionality and/or size of the template, quantum (size) effects may appear for some types of materials. In order to check for possible quantum effects for *h*-BN, as modeled in the present investigation, test calculations were performed involving adsorption of gaseous H to various di-

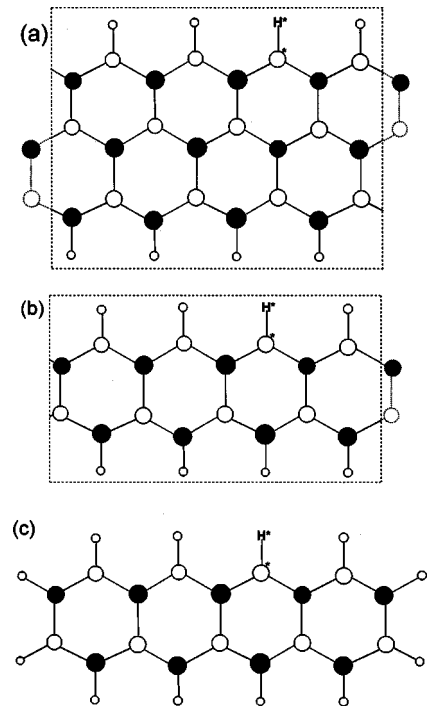


FIG. 4. An illustration of the (a) large two-dimensional slab model, (b) small two-dimensional slab model, and (c) cluster model, used for the test calculations. Only the asterisk-marked atoms are allowed to relax.

mensions of an *h*-BN model. The total energies for the different templates were obtained using the program system CASTEP from Biosym/Molecular Simulation Technologies of San Diego. The levels of theory used were the gradient-corrected GGA for closed-shell systems, and the GGS for radical systems (both developed by Perdew and Wang).³⁰ The calculations were fully self-consistent with eigenvalues obtained using two k points, generated according to the Monkhorst-Pack scheme,³¹ which produces a uniform mesh of k points in the reciprocal space. This specific number of k points has, in an earlier work by two of the authors, been found to be adequate in studying the nucleation of diamond on edge atoms of *h*-BN (001).²⁶

Three different models were used. The largest one is a two-dimensional slab, which is extended infinitesimally in one direction (x axis). It is here modeled by a unit cell that is translated in the x , y , and z directions during the calculation. Each unit cell contains one layer of eight B_3N_3 rings fused together and terminated with hydrogen atoms in the third direction (z axis) [Fig. 4(a)]. The medium-sized model is also a two-dimensional slab extended infinitesimally in one direction. The only difference is that this unit cell contains one layer of *four* (instead of eight) B_3N_3 rings fused together [Fig. 4(b)]. The smallest model in the test calculations is a three-dimensional cluster, identical to the model used in the present investigation, i.e., four aligned B_3N_3 rings terminated with H atoms [Fig. 4(c)]. It must also be stressed that the three models do not only represent different sizes, they also represent a successively increased terminating species over BN ratio when going from the larger to the smaller model.

The adsorbed hydrogen atom and the edge atom bonding to it were, for all models used, allowed to fully relax during the geometry optimization.

The resulting energies for adsorption of H to the B-rich (100) edge were 462, 466, and 460 kJ/mol for the large, medium, and small models, respectively. Thus, the adsorption energies only differ by less than about 1%, upon reducing the dimensionality and size of the model system (as well as changing the H/BN ratio). On the N-rich (100) edge, the adsorption energies were 493, 488, and 504 kJ/mol for the large, medium, and small models, respectively. On this edge, the difference in adsorption energy is thus somewhat larger than on the (100) edge, however, very small and less than about 2%–3%. It can therefore be concluded that the small-cluster model is computationally valid in the present investigation. This conclusion is also strongly supported by earlier investigations and test calculations by the present authors regarding H and F adsorption on *c*-BN(111) surfaces.^{32,33} Furthermore, quantum effects are generally only expected to be important for semiconducting materials with a sufficiently small band gap, e.g., for Cd₃As₂ with a band gap of 0.13 eV.³⁴ For CdS with a band gap of 2.42 eV, on the other hand, the quantum effects are appreciably smaller.³⁴ Hexagonal BN has an optical band gap of about 5.2 eV,³⁵ and, hence, no larger size effects on the band gap can be expected.

IV. RESULTS AND DISCUSSION

A. Nucleation on the zigzag edges of the basal plane

1. General

In a previous paper by the present authors, the *h*-BN(001) plane was investigated as a provider of nucleation sites for *c*-BN growth.¹⁵ The investigation is now continued with the nucleation on the *h*-BN(001) plane edges. It is then of special interest to investigate the possibility to be able to control the growth of *c*-BN by nucleating on *h*-BN. As was discussed in the Introduction, *sp*²-hybridized BN will be produced in both the chemical and physical routes of BN thin-film deposition. The mechanism of the *c*-BN nucleation is assumed to involve adsorption of B- or N-containing species (e.g., BF₃, NH₃), as well as abstraction of terminating H or F species. The individual steps are then also assumed to result in the completion of a six-member ring (buckled or planar) of alternating boron and nitrogen atoms. The details in the various mechanisms are not explicitly studied within the present investigation. What has been of most interest is instead the difference in total energy for the corresponding buckled and planar outgrowths.

For the situation with a partly buckled ring, the *sp*²-hybridized atoms in the ring originate from the edge atoms and the saturated atoms constitute the actual outgrowth [Fig. 2(a)]. The corresponding planar outgrowth (representing a continuous growth of *h*-BN) can also be described as a three atomic part, which, together with the three *sp*²-hybridized edge atoms, leads to the completion of a new planar B₃N₃ ring [Fig. 2(b)]. The outgrowth representing a continued *h*-BN growth will on the N-rich (100) edge fit into an aromatic system with alternating single and double bonds

TABLE I. Relative energies obtained for the nucleation of buckled ring systems and their planar counterparts on the (100) zigzag edge of the *h*-BN basal plane.

Planar outgrowth	Buckled outgrowth	ΔE (kJ/mol)
BN ₂ H ₃ H substituted	BN ₂ H ₅ H substituted	329
F substituted	F substituted	339
BN ₂ F ₃ H substituted	BN ₂ F ₅ H substituted	466
F substituted	F substituted	520

(a B-N=B skeleton, with hydrogen atoms omitted for clarity). All three atoms of the outgrowth are in this case *sp*² hybridized. On the B-rich (100) edge, however, there will be a surplus of two electrons resulting in a lone pair of electrons situated on the N(1) atom in the N(1)-B=N(2) outgrowth. The hybridization will therefore be *sp*³, *sp*², and *sp*² for the N(1), B, and N(2) atoms, respectively. Moreover, the two terminating species (H and F) were, in the present investigation, chosen to represent two “extremes.” Fluorine is the most electronegative of the elements (electronegative (F) = 3.98), which, hence, possesses a higher electron withdrawing ability compared to hydrogen. The latter is a more moderate terminating species (electronegative (H) = 2.2).³⁶ Furthermore, both species are commonly used in many CVD processes of BN.

2. B-rich (100) edge

As can be seen in Table I, the growth of partially saturated (buckled) ring systems on the B-terminated (100) edge are for all different outgrowths investigated, energetically favorable compared to the planar counterparts. For the H-terminated (100) edge, the NBN planar H-terminated outgrowth is less stable than the saturated buckled counterpart by 329 kJ/mol. The same order of stability is observed for an F-terminated (100) edge. There is then a favoring of the saturated outgrowth by as much as 520 kJ/mol. In an earlier investigation concerning diamond nucleation on terminated *h*-BN(001) zigzag edges, it was concluded that neither electronegative (F or OH), electropositive (Na), nor bulky (CH₃) neighboring terminating species had a large effect on the difference in energy between a buckled and a planar outgrowth.^{26,27} In contrast to diamond, boron nitride is a polar compound. The question is now, how is the nucleation of *c*-BN affected by different neighboring terminating species (with varying electronegativities)? From here on in the text, there will for simplicity be a different terminology for species terminating outgrowths, compared to species terminating the neighboring edge atoms. They will be called terminators vs substituents. In order to investigate the eventual influence of edge substitution, a mixture of type of substitution and termination has been studied in the present paper. When using the combination of H termination and F substitution, the relative energy for the buckled outgrowth was 339 kJ/mol. The corresponding result for the combination of F termination and H substitution was 520 kJ/mol. These results are very similar to the situation with identical terminating and substituting species. The differences are for H termina-

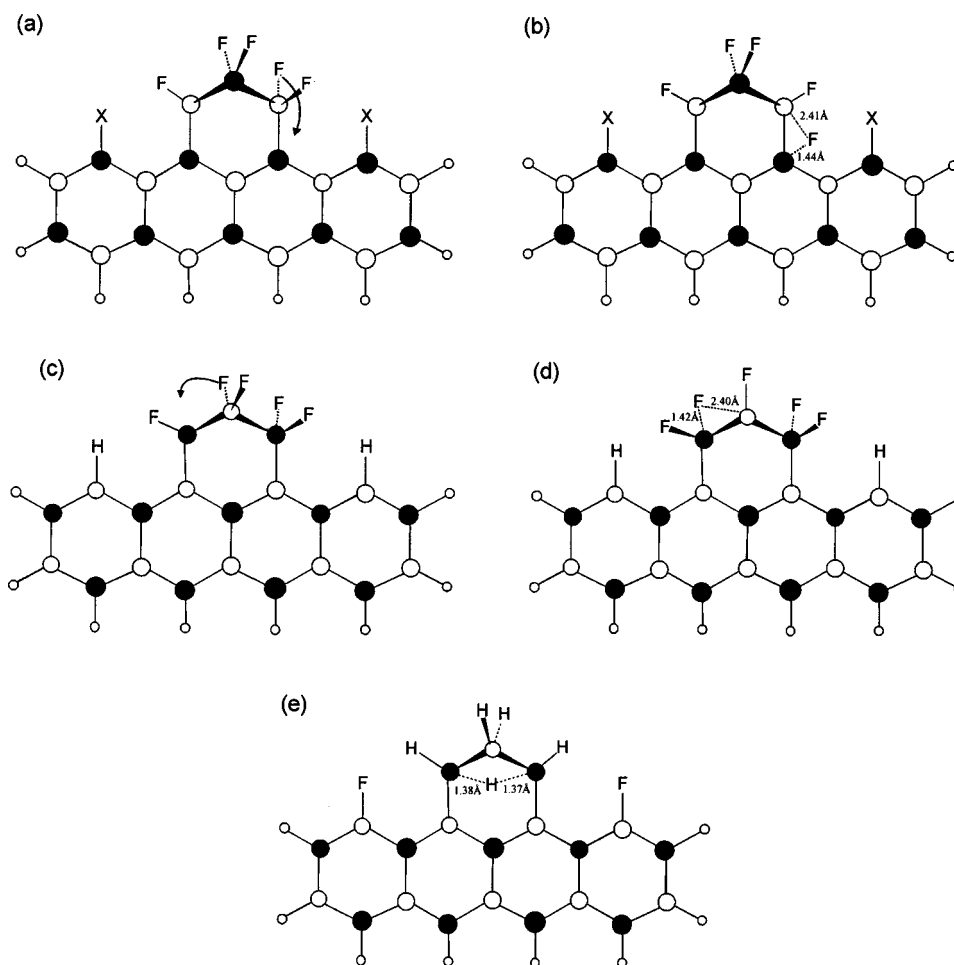


FIG. 5. Terminating F species move from an “N” to a “B” position as a result of the geometry optimization; (a) and (b) The N-rich ($\bar{1}00$) edge and, (c) and (d) the B-rich (100) edge. (e) represents the H-terminated outgrowth on the ($\bar{1}00$) edge and shows the two-electron-three-center B H B bond. The angle $\angle\text{BHB}$ is 90.1° .

tion 10 kJ/mol (329 vs 339 kJ/mol) and for F termination 54 kJ/mol (466 vs 520 kJ/mol). It can thus be seen that the stability of the cubic nuclei (by using H or F substituents) is not significantly altered for either of the two differently terminated outgrowths (H or F). Hence, the atoms neighboring the outgrowth do not significantly affect the stability of the nucleation of *c*-BN.

The large difference in stability observed for the F-terminated outgrowths compared to the corresponding H-terminated ones (~ 490 vs ~ 330 kJ/mol) is found to be strongly correlated to differences in the geometrical structure. As a result of the geometry relaxation, the axial F atom originally bonded to the N(2) atom in the buckled N(1)BN(2) outgrowth was found to bend backwards to form a bond with the (100) B edge [Fig. 5(a)]. As can be seen in Fig. 5(b), the resulting B-F and N(2)-F bond lengths are 1.44 and 2.41 Å, respectively. Since the N-F bond is weaker than the corresponding B-F bond (343 vs 757 kJ/mol),^{37,38} the transition from N-F to B-F implies that the “buckled” system becomes relatively more stable. The H-terminated outgrowths, for which there are no such geometrical rearrangements, do not have the driving force to invoke a transition from N-H to B-H. The difference in bond energy between N-H and B-H is

too small and has reversed order (≤ 339 vs 333.9 kJ/mol).^{37,39}

The angles between the atoms constituting the buckled outgrowths were measured and averaged. The deviation from a tetrahedron angle (109.5°) was used as an indication of how close to sp^3 the resulting hybridization of the atoms were. The absolute value of the deviation did not, with one exception, exceed four degrees for any of the different outgrowths (F or H terminated) on the different edges investigated. The F-terminated cubic outgrowth on the (110) edge showed a deviation of $+5.7^\circ$. A plausible explanation for this is the strong interaction of the F atoms (on the outgrowth) with the B and N atoms situated on the edge. This may then induce geometrical constraints in the outgrowth representing the chair (cubic) conformation (see Sec. IV B).

3. N-rich ($\bar{1}00$) edge

The relative energies for the different outgrowths on the N-rich ($\bar{1}00$) edge are shown in Table II. In analogy to the B-rich (100) edge, the growth of the partially saturated (buckled) ring system is energetically favored versus the continuous growth of *h*-BN.

TABLE II. Relative energies obtained for the nucleation of buckled ring systems and their planar counterparts on the (100) zigzag edge of the *h*-BN basal plane.

Planar outgrowth	Buckled outgrowth	ΔE (kJ/mol)
B ₂ NH ₃ H substituted	B ₂ NH ₃ H substituted	336
F substituted	F substituted	414
B ₂ NF ₃ H substituted	B ₂ NF ₃ H substituted	630
F substituted	F substituted	476

For the H-terminated and H-substituted type of outgrowth, the relative energy for the buckled outgrowth is 336 kJ/mol. For the F-terminated and F-substituted outgrowth, there is a relative energy of 476 kJ/mol. The difference between the two types of termination is somewhat smaller on this edge than it is on the B-rich edge (140 vs 191 kJ/mol, respectively). In conformity with the B-rich (100) edge, the situation with a mixture of termination and substitution was calculated. The relative energy for a buckled H-terminated outgrowth on an F-substituted edge is 414 kJ/mol, and is thus higher by ~ 80 kJ/mol compared to the situation with H as both terminator and substituent (336 kJ/mol). For the other situation, with F termination and H substitution, there is a relative energy of 630 kJ/mol, which is ~ 150 -kJ/mol higher than the situation with F termination and F substitution (476 kJ/mol). In contrast to the (100) edge, it can thus be seen that different substitution on the ($\bar{1}00$) edge alters the relative stabilization energy for both H- and F-terminated outgrowths. For the H-terminated and F-substituted case, the increased stability correlates to the geometry. In Fig. 5(e), it can be seen that a three-center-two-electron ($3c-2e$) bond is formed as a result of the geometry optimization. The angle $\angle BHB$ is 90.1° (the value for β -diborane)⁴⁰ and the bridging B-H bond distances are 1.37 and 1.38 Å, respectively [the value for gaseous diborane (1.37 ± 1 Å)].⁴¹

As for the (100) edge, changes in the geometry of the F-terminated outgrowths occur on the ($\bar{1}00$) edge, albeit only for the H-substituted situation. This strongly correlates to differences in stability between the H- and F-substituted outgrowths (~ 480 vs 630 kJ/mol). The equatorial F atom bonded to the N atom in the B(1)NB(2) outgrowth migrates to the B(1) atom as a result of the structural optimization procedure [Fig. 5(c)]. The numerical values of B(1)-F and N-F bond lengths (1.42 vs 2.40 Å) illustrate this [Fig. 5(d)]. A symmetric outgrowth is consequently formed [B(1)F₂-NF-B(2)F₂]. In analogy to the B-rich (100) edge, the transition from N-F to B-F leads to a more stable buckled system due to the different B-F and N-F bond strengths.^{37,39} On the H-terminated outgrowths, no such transition (N-H to B-H) occurs.

B. Nucleation on the armchair edge of the basal plane

There are two possible conformations of the sp^3 -hybridized (buckled) outgrowth from the (110) armchair edge of the *h*-BN basal plane. One is the chair conformation [Fig. 3(a)] and the other is the boat conformation [Fig. 3(b)]. The chair configuration corresponds to a cubic (*c*-BN)

TABLE III. Relative energies obtained for the nucleation of buckled ring systems and their planar counterparts on the (110) armchair edge of the *h*-BN basal plane.

Planar outgrowth	Buckled outgrowth	ΔE (kJ/mol)
BNH ₂	BNH ₄ <i>c</i> -BN	576
	<i>w</i> -BN	725
BNF ₂	BNF ₄ <i>c</i> -BN	820
	<i>w</i> -BN	858

nucleus, whereas the boat configuration corresponds to a wurtzitic (*w*-BN) nucleus. Figure 3(c) illustrates the continued growth of *h*-BN and consists of only sp^2 -hybridized atoms.

The process of BN nucleation on the armchair edge of the *h*-BN basal plane is thought to occur with a similar process as on the zigzag edges (see Sec. IV A 1). However, the two edge atoms (one B and one N) that are bonding to the outgrowth must also be sp^3 hybridized in order to achieve the right geometrical structure for the buckled outgrowth [Figs. 3(a) and 3(b), respectively]. In the relative energy calculation for the armchair edge, Eq. (1) must, hence, be balanced by $+2E_H$ (E_H = total energy of an H atom) in addition to the total energy of two terminating atoms ($+2E_X$). All atoms in the outgrowth, as well as the two extra hydrogen atoms on the edge, are allowed to fully relax during the geometry optimization.

The difference in total energy between the planar and the two buckled types of outgrowths (chair or boat conformation) from the armchair edge is presented in Table III. The results show that the buckled outgrowths are in all cases energetically preferred over the planar counterpart, which represents a continued growth of hexagonal boron nitride. The relative energy obtained for the H-terminated outgrowths in the chair (*c*-BN) and boat (*w*-BN) conformations is 576 and 725 kJ/mol, respectively. The numerical values of the relative energy for the corresponding F-terminated outgrowths are 820 and 858 kJ/mol, respectively. Hence, the fluorine atoms contribute also for this type of edge to the higher stability for the buckled outgrowths. Noticeably, the difference in stability between the differently terminated outgrowths (H or F) is almost twice as large for the chair conformation [246 kJ/mol (576 vs 820 kJ/mol)] than for the boat conformation [133 kJ/mol (725 vs 858 kJ/mol)]. As presented above, boat nuclei are more stable than the corresponding chair nuclei. The difference in relative energy is 149 kJ/mol for the H-terminated outgrowths and 38 kJ/mol for the F-terminated ones. However, the energy difference of 38 kJ/mol between the two different nucleus conformations is not large enough to be able to draw any conclusions regarding phase stability. The somewhat larger difference of 149 kJ/mol suggests that the wurtzitic nuclei are more stable than the cubic ones.

The order of stability is generally regarded to be very interesting. A qualitative comparison of our theoretical observations with calculations of total energy for the two types of bulk structures will reveal the more established stability order: *c*-BN is more stable than *w*-BN. A direct quantitative

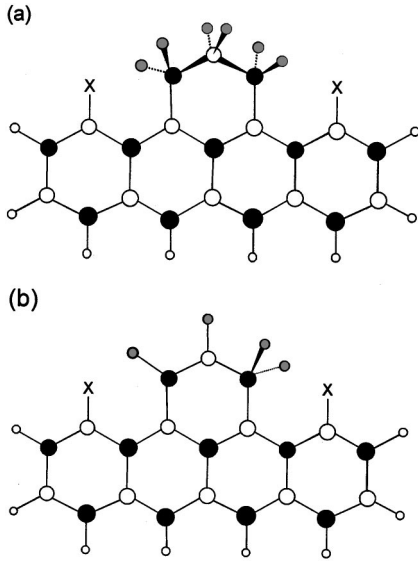


FIG. 6. An illustration of (a) *c*-BN and (b) *h*-BN nucleation on the $(\bar{1}00)$ edge in an extremely radical-rich environment. The gray atoms are either terminating H or F species. The terminating species “X” (neighboring the outgrowth) are either H or F.

comparison between our results and the results obtained by other research groups would, however, be misleading since the values presented here are calculated as an energy per mol template (including all of its atoms). If the values are instead recalculated as energy per mol atoms (by dividing by the 30 atoms of the template), interesting results will be obtained. For the H-terminated outgrowths, the energy difference between *c*-BN and *w*-BN will then become 5.0 kJ/(mol atoms) and for the F-terminated case, it will be 1.3 kJ/(mol atoms) (both in favor of *w*-BN). Earlier theoretical investigations, using either pseudopotentials with plane-wave basis sets or an *ab initio* orthogonalized linear combination of atomic orbitals method, have shown that the cubic phase is favored over the wurtzitic by 1.9 and 0.5 kJ/(mol atoms), respectively.^{42,43} A qualitative comparison of energies shows that our results, concerning phase stability within the nucleation stage, are numerically very similar to the results obtained from the bulk-structure stability investigations. However, since the absolute numerical values of the energies are very small, our obtained (and reversed) order of stability for *c*-BN and *w*-BN will most probably be the effect of using different theoretical methods and approximations therein.

C. Nucleation in extremely reactive environments

As a test of the behavior of BN growth in an extremely reactive and radical-rich environment, the hypothesis of extra adsorption of H or F to the various outgrowths is investigated. In the BNB case, this will lead to the production of an *ionic* $[B(X_2)-N(X_2)-B(X_2)]$ and $[B(X)-N(X)-B(X_2)]$ type of outgrowth for the buckled and planar outgrowths, respectively. The relative energy for the ionic case will here be compared to the relative energy for the more likely *neutral* situation. For the NBN outgrowth, on the other hand, the adsorption of an extra species leads to the formation of a

TABLE IV. Relative energies obtained for the nucleation in extremely reactive environments of buckled ring systems and their planar counterparts on the (100) edge of *h*-BN (001).

Planar outgrowth	Buckled outgrowth	ΔE (kJ/mol)
BN ₂ H ₄ H substituted	BN ₂ H ₆ H substituted	439
F substituted	F substituted	448
BN ₂ F ₄ H substituted	BN ₂ F ₆ H substituted	434
F substituted	F substituted	552

radical $[N(X_2)-B(X_2)-N(X_2)]$ or $[N(X)-B(X)-N(X_2)]$ type of outgrowth. The relative energy for these radical outgrowths will, in the present study, be compared to the *non-radical* situation. If the adsorption does occur, it is thought to be of an extremely short-lived character. The ionic cubic and hexagonal outgrowths are shown in Figs. 6(a) and 6(b), respectively.

The relative energies for the radical buckled outgrowths on the B-rich (100) edge are presented in Table IV. They are to be compared with the relative energies for the nonradical buckled outgrowths in Table I H-terminated and H-substituted as well as F-terminated and F-substituted outgrowths have then been investigated. Moreover, in conformity with Secs. IV A 1–3, the method of mixed termination and substitution was also employed. The difference in relative energy for a radical and a nonradical situation is for the H-terminated outgrowths ~ 110 kJ/mol in favor of the radical situation [439 vs 329 H substituted) and 448 vs 339 (F substituted) kJ/mol]. For the F-terminated outgrowths, the corresponding difference is ~ 30 kJ/mol (434 vs 466 and 552 vs 520 kJ/mol). This implies a weak tendency for the H-terminated nonradical outgrowths (both H and F substituted) to adsorb an extra radical H species and, hence, become a radical outgrowth. On the other hand, there is hardly any tendency for F-terminated nonradical outgrowths to undergo any further adsorption of radical F species.

The relative energies for the ionic buckled outgrowths from the N-rich $(\bar{1}00)$ edge are presented in Table V. These values will be compared with the numerical values for the neutral outgrowths in Table II. It can then be seen that all differences in relative energy between ionic and neutral buckled outgrowths lie within the range $+78$ – -59 kJ/mol. Interestingly, it is only the two situations with identical species for termination and substitution (H/H and F/F) that are energetically in favor of the adsorption of radical H or F species to a neutral outgrowth ($+78$ vs $+40$ kJ/mol). How-

TABLE V. Relative energies obtained for the nucleation in extremely reactive environments of buckled ring systems and their planar counterparts on the (100) edge of *h*-BN (001).

Planar outgrowth	Buckled outgrowth	ΔE (kJ/mol)
B ₂ NH ₄ H substituted	B ₂ NH ₆ H substituted	414
F substituted	F substituted	385
B ₂ NF ₄ H substituted	B ₂ NF ₆ H substituted	571
F substituted	F substituted	516

ever, these differences in relative energy are numerically very small. Moreover, they are expected to become even smaller at the temperatures used in chemical vapor deposition of *c*-BN thin films.

As a result of these calculations, it will be possible to draw the conclusion that both neutral as well as ionic/radical types of outgrowths will thermodynamically have the same probability to form on the edges of the *h*-BN basal plane in an extremely radical-rich environment. Hence, this will further support the idea of nucleation and growth of *c*-BN on *h*-BN.

V. CONCLUSION

The nucleation of cubic BN on the zigzag edges (100) and $\bar{1}00$ as well as on the armchair edge (110) of the basal plane of hexagonal BN has been theoretically investigated using a cluster approach and density-functional theory (DFT). The total energy of the different buckled (cubic and wurtzitic) outgrowths from the edge atoms has been related to the total energy of the corresponding planar (hexagonal) counterpart.

The outgrowths on the different edges were either H or F terminated. The result of the calculations show that in an H- or F-rich environment, the nucleation of *c*-BN along the zigzag edges as well as along the armchair edge of *h*-BN(001) is energetically more favorable than a corresponding nucleation of *h*-BN. On the armchair edge, the nucleation of *w*-BN is even more energetically preferred than the nucleation of *c*-BN. The hybridization of the atoms constituting the cubic and wurtzitic outgrowths was close to sp^3 in all cases but one, since the deviations from the tetrahedron angle were less than four degrees. The species H or F, terminating the edge atoms closest to the different outgrowths, were shown to have only a minor effect on the relative nucleation stability.

The effectiveness of the terminating species H and F in stabilizing the cubic nuclei of BN was investigated by comparing the total energies for terminated outgrowths. It was shown that the F-terminated outgrowths are more stable than

the corresponding H-terminated ones for all edges investigated. The differences in stability (in relation to H-terminated outgrowths) are ~ 160 , ~ 180 , and ~ 190 kJ/mol for the edges (100), $\bar{1}00$, and (110), respectively.

Moreover, the following order of cubic stability was observed for the various edges (for both H and F termination): $(110) \gg (\bar{1}00) > (100)$. The differences in stability between the (110) and $\bar{1}00$ edges are 200 and 270 kJ/mol for H- and F-terminated outgrowths, respectively. The corresponding differences between the $\bar{1}00$ and (100) edges are 40 and 60 kJ/mol, respectively. It should be stressed that only the numerical difference in total energy between cubic and hexagonal nuclei is presented here. The results in the present study, hence, predict the phase that will be the thermodynamically most plausible if any nucleation may occur. In order to study the possibility for any nucleation to form (both thermodynamically and kinetically) one has to look for specific reaction mechanisms with accompanying transition states. This is planned to be our next step within this area of research.

In the situation with an extremely radical-rich environment, a second type of both buckled and planar outgrowths has been modeled. It was then observed that, with one exception, there is an equal probability to obtain either a neutral or a radical/ionic outgrowth in the CVD growth of *c*-BN. The nonradical H-terminated outgrowths on the B-rich (100) edge showed a weak tendency for adsorbing an extra radical H species and, hence, become radical outgrowths. This result strongly supports a favored *c*-BN nucleation on *h*-BN.

ACKNOWLEDGMENTS

This work was supported by the Swedish Research Council for Engineering Sciences (TFR) and the Ångström Consortium. Computational results were obtained using software programs from Biosym Technologies of San Diego—first-principles DFT calculations from DMOL and graphic display using INSIGHT II.

¹I. Konyashin, J. Bill, and F. Aldinger, *Chem. Vap. Deposition* **3**, 239 (1997), and references therein.

²D. L. Medlin, T. A. Friedmann, P. B. Mirkarimi, G. F. Cardinale, and K. F. McCarty, *J. Appl. Phys.* **79**, 3567 (1996).

³D. J. Kester and R. Messier, *J. Appl. Phys.* **72**, 504 (1992).

⁴P. B. Mirkarimi, K. F. McCarty, D. L. Medlin, W. G. Wolfert, T. A. Friedmann, and E. J. Klaus, *J. Mater. Res.* **9**, 2925 (1994).

⁵D. J. Kester, K. S. Ailey, R. F. Davis, and K. L. More, *J. Mater. Res.* **8**, 1213 (1993).

⁶M. F. Plass, W. Fukarek, A. Kolitsch, N. Schell, and W. Möller, *Thin Solid Films* **305**, 172 (1997).

⁷W.-L. Zhou, Y. Ikuhara, M. Murakawa, S. Watanabe, and T. Suzuki, *Appl. Phys. Lett.* **66**, 2490 (1995).

⁸P. Widmayer, H.-G. Boyen, P. Ziemann, P. Reinke, and P. Oelhafen, *Phys. Rev. B* **59**, 5233 (1999).

⁹A. Bartl, S. Bohr, R. Haubner, and B. Lux, *J. Ref. Hard Metals* **14**, 145 (1996).

¹⁰S. P. S. Arya and A. D'Amico, *Thin Solid Films* **157**, 267 (1988), and references therein.

¹¹E. Yamaguchi, *Mater. Sci. Forum* **54–55**, 329 (1990).

¹²X. Ma, J. Yang, D. He, and G. Chen, *Thin Solid Films* **322**, 37 (1998).

¹³C. A. Taylor II and R. Clarke, in *III-Nitride, SiC and Diamond Materials for Electronic Devices*, edited by D. K. Gaskill, C. D. Branat, and R. J. Nemanich, MRS Symposia Proceedings No. 423 (Materials Research Society, Pittsburgh, 1996), p. 265.

¹⁴J. L. Andújar, E. Bertran, and Y. Maniette, *Diamond Relat. Mater.* **6**, 589 (1997).

¹⁵B. Mårlid, K. Larsson, and J.-O. Carlsson, *J. Phys. Chem.* **103**, 7637 (1999).

- ¹⁶P. Hohenberg and W. Kohn, Phys. Rev. B **136**, 864 (1964).
- ¹⁷W. Kohn and L. J. Sham, Phys. Rev. A **140**, 1133 (1965).
- ¹⁸A. J. Becke, J. Chem. Phys. **88**, 2547 (1988).
- ¹⁹C. Lee, W. Yang, and R. Parr, Phys. Rev. B **37**, 785 (1988).
- ²⁰R. Colle and O. Salvetti, Theor. Chim. Acta **37**, 329 (1975).
- ²¹J. P. Perdew, J. A. Chevary, S. H. Vosko, K. A. Jackson, M. R. Pederson, D. J. Singh, and C. Fiolhais, Phys. Rev. B **46**, 6671 (1992).
- ²²W.-L. Zhou, Y. Ikuhara, M. Murakawa, S. Watanabe, and T. Suzuki, Appl. Phys. Lett. **66**, 2490 (1995).
- ²³K. P. Hubert and G. Herzberg, in *Molecular Spectra and Molecular Structure Constants of Diatomic Molecules* (Van Nostrand, New York, 1979).
- ²⁴W. J. Hehre, L. Radom, P. V. R. Schleyer, and J. A. Pople, in *Ab Initio Molecular Orbital Theory* (Wiley, New York, 1986).
- ²⁵E. Johansson, K. Larsson, and J.-O. Carlsson, J. Phys. Chem. **99**, 12 781 (1995).
- ²⁶M. Carbone, K. Larsson, and J.-O. Carlsson, J. Phys. Chem. A **101**, 9445 (1997).
- ²⁷M. Carbone, K. Larsson, and J.-O. Carlsson, J. Phys. Chem. B **102**, 5866 (1998).
- ²⁸S. P. Mehandru, A. B. Andersson, and J. C. Angus, J. Phys. Chem. **96**, 10 978 (1992).
- ²⁹R. S. Pease, Acta Crystallogr. **5**, 356 (1952).
- ³⁰J. P. Perdew and Y. Wang, Phys. Rev. B **45**, 13 244 (1992).
- ³¹H. J. Monkhorst and J. D. Pack, Phys. Rev. B **13**, 5188 (1976).
- ³²B. Mårilid, K. Larsson, and J.-O. Carlsson, Phys. Rev. B **60**, 16 065 (1999).
- ³³K. Larsson and J.-O. Carlsson, J. Phys. Chem. B **103**, 6533 (1999).
- ³⁴R. J. D. Miller, G. L. McLendon, A. J. Nozik, W. Schmickler, and F. Willig, in *Surface Electron Transfer Processes* (Wiley, New York, 1995).
- ³⁵E. Yamaguchi, Mater. Sci. Forum **54–55**, 329 (1990).
- ³⁶D. F. Shriver, P. W. Atkins, and C. H. Langford, in *Inorganic Chemistry* (Oxford University Press, Oxford, 1994).
- ³⁷K. P. Hubert and G. Herzberg, in *Molecular Spectra and Molecular Structure Constants of Diatomic Molecules* (Van Nostrand, New York, 1979).
- ³⁸K. H. Lau and D. L. Hildenbrand, J. Chem. Phys. **72**, 4928 (1980).
- ³⁹J. W. C. Jones, F. A. Grimm, and R. F. Porter, J. Mol. Spectrosc. **22**, 435 (1967).
- ⁴⁰H. W. Smith and W. N. Lipscomb, J. Chem. Phys. **43**, 1060 (1965).
- ⁴¹B. V. Nekrasov and V. V. Shtutser, Zh. Obshch. Khim. **18**, 832 (1948).
- ⁴²J. Furthmüller, J. Hafner, and G. Kresse, Phys. Rev. B **50**, 15 606 (1994).
- ⁴³Y.-N. Xu and W. Y. Ching, Phys. Rev. B **44**, 7787 (1991).